Neural network models of peak temperature, torque, traverse force, bending stress and maximum shear stress during friction stir welding

V. D. Manvatkar[1], A. Arora[2], A. De*[1] and T. DebRoy[2]

Tool and workpiece temperatures, torque, traverse force and stresses on the tools are affected by friction stir welding (FSW) variables such as plate thickness, welding speed, tool rotational speed, shoulder and pin diameters, pin length and tool material. Because of the large number of these welding variables, their effects cannot be realistically mapped by experiments. Here, we develop, test and make available a set of five neural networks to calculate the peak temperature, torque, traverse force and bending and equivalent stresses on the tool pin for the FSW of an aluminium alloy. The neural networks are trained and tested with the results from a well tested, comprehensive, three-dimensional heat and material flow model. The predictions of peak temperature and torque are also compared with appropriate experimental data for various values of shoulder radius and tool revolutions per minute. The models can be used even beyond the range of training with predictable levels of uncertainty.

Keywords: Friction stir welding, Neural network model, Peak temperature, Traverse force, Torque, Stresses

Introduction

Friction stir welding (FSW) has gained widespread commercial applications in the recent past, particularly for the welding of soft alloys.[1,2] Process monitoring and control often involve monitoring several variables such as workpiece and tool temperatures, torque and traverse force. These monitoring variables and the quality of the welds are affected by welding variables such as tool geometry, tool material and rotational speed, welding speed, workpiece thickness and thermophysical properties. In view of the large number of variables and the complexity of the welding process, no generally usable relationship between the monitoring variables and the welding variables has emerged. Currently available methods to quantitatively understand the role of welding variables include the use of comprehensive models of heat transfer and materials flow,[3–11] correlations based on dimensional analysis[12,13] and simplified analytical correlations.[13] Comprehensive models are rigorous but time consuming and therefore unsuitable for real time applications or where large volumes of results are needed. Most correlations based on dimensional analysis are suitable for interrogating trends of variation of variables but not their exact values. Simplified analytical models are insightful but lack the generality and accuracy of the comprehensive models.

Artificial neural networks (ANNs) are used to solve complex welding problems,[14–16] where the form of the relationship among the variables is not explicitly known. Familiar examples of neural network based calculations in FSW involve estimation of grain size,[17,18] joint misalignment and seam tracking,[19] prediction of worm-hole defects[20] and mechanical properties such as shear stress,[21] tensile stress,[22] fatigue life,[23] hardness[24] and ductility.[24] A common feature of the previous works on the ANNs of the FSW process is that the networks are trained with experimental data. Here, we report the development of neural networks to calculate the peak temperature, torque, traverse force, bending stress and maximum shear stress experienced in the tool during FSW. The peak temperature, torque and traverse force provide useful process insight and also serve as process control parameters, and the stresses on the tool provide an understanding of the thermomechanical conditions experienced by the tools.

The numbers of input and output variables of an ANN determine the volume of data required to train the neural network. For FSW, since a large number of variables affect the peak temperature, torque and traverse force, it is a difficult task to obtain these results experimentally. Furthermore, the stresses on the tool cannot be easily measured experimentally. A recourse is to obtain the training data from a well tested comprehensive numerical

[1]Department of Mechanical Engineering, IIT Bombay, Mumbai, Maharashtra, India
[2]Department of Materials Science and Engineering, The Pennsylvania State University, University Park, PA, USA

*Corresponding author, email de.amitava1967@gmail.com

Published by Maney on behalf of the Institute
Received 19 March 2012; accepted 19 April 2012
DOI 10.1179/1362171812Y.0000000035

heat transfer and material flow model. Since the numerical heat transfer and material flow model has been well tested with experimental data, the results of the model provide reproducible data that conform to the basic phenomenological laws within the limits of the accuracy of the calculations. Because of the recent improvements in the computational hardware and software, a large volume of training and testing data can be generated in a realistic time frame.

Here, we report the development and testing of a set of five neural networks to calculate peak temperature, torque, traverse force and bending and equivalent stresses on the tool pin for the FSW of aluminium alloy 7075. The training and testing data for the neural networks are obtained from a well tested, comprehensive, three-dimensional heat and materials flow model. The procedure allows the estimation of uncertainties in the predicted values of all variables. Furthermore, the quality of the predictions of peak temperature and torque is also examined by comparing with appropriate available experimental data for various values of shoulder radius and tool revolutions per minute.

Numerical model

A well tested, three-dimensional, heat transfer and viscoplastic material flow model for FSW is used to compute the temperature field, traverse force and torque during welding.[7–12] The model solves the equations of conservation of mass, momentum and energy in steady state, three-dimensional Cartesian coordinate system considering incompressible single phase flow. The numerical model has been explained in detail in several previous publications[7–12] and is not repeated here. The bending stress and the maximum shear stress on the tool are estimated following analytical relations from solid mechanics and using the computed results of temperature field, torque and the distribution of force along the tool pin length.[25] A brief outline of the methodology to estimate the bending stress and maximum shear stress on the tool pin is presented here for completeness.

Because of the linear motion (welding speed) of the FSW tool, the tool pin will experience normal force in the direction opposite to the direction of welding. The force would be higher towards the bottom of the pin as the material away from the tool shoulder is colder and hence stronger. In effect, the tool pin, which is fixed only with the shoulder and free for the rest of the length, will experience a bending stress, σ_B, that can be estimated as[25]

$$\sigma_B = \frac{4\cos\theta}{\pi r^3}\int_{z_1}^{L} zq(z)\mathrm{d}z \tag{1}$$

where r and L are the pin radius and length respectively, θ is the angle of any point on the pin profile with the welding direction, $q(z)$ is the typical force distribution on the tool pin acting normal to the axis of the pin and in a direction opposite to the welding speed and z_1 is the distance of the point from the fixed end of the pin. The shear stress, τ_B, at any point on the pin profile due to bending can be estimated as[25]

$$\tau_B = \frac{4}{3}\frac{\sin^2\theta}{\pi r^2}\int_{z_1}^{L} q(z)\mathrm{d}z \tag{2}$$

Furthermore, the rotational motion of the tool pin through the viscous material will result in a shear stress, τ_T, that can be estimated as[25]

$$\tau_T = \frac{\oint_A r_A \times (1-\delta)\tau \times \mathrm{d}A}{\pi r^3/2} \tag{3}$$

where the numerator depicts the sticking torque with δ the spatial fractional slip,[7–12,25] r_A the distance of any infinitesimal area element $\mathrm{d}A$ from the tool axis and τ the temperature dependent shear strength of the workpiece material. The resultant maximum shear stress τ_{max} at any point on the tool profile can finally be estimated following Tresca's yield criterion[25]

$$\tau_{max} = \left[\left(\frac{\sigma_B}{2}\right)^2 + (\tau_B + \tau_T\sin\theta)^2 + (\tau_T\cos\theta)^2\right]^{1/2} \tag{4}$$

Equations (1)–(4) are used to estimate the bending stress and the maximum shear stress experienced by the tool during the FSW process.

Artificial neural network model

A set of ANN models are developed to understand the effect of the welding conditions and tool dimensions on the peak temperature, torque, traverse force and stresses on the tool pin during FSW of AA 7075. The training and testing data sets for the ANN models are generated using the heat transfer and viscoplastic flow model (for temperature, torque and traverse force) and further using equations (1) and (4) respectively for bending stress and maximum shear stress. All the thermophysical material properties required for numerical model calculations are considered temperature dependent.[10] The training and testing data sets consist of 124 and 49 different combinations of welding conditions and the corresponding response variables respectively. The combinations of welding conditions in the training data set are decided following Taguchi's L50 array and central composite rotatable design (CCD) and using five levels each of the six welding conditions in both cases.[26] The combinations of welding conditions in the testing data set are decided based on Taguchi's L50 array and using five levels each of the six welding conditions. Table 1 depicts various levels and ranges of the input welding conditions considered for the training and testing of ANN models.

Figure 1 is a schematic diagram of the neural network models that are developed in the present work. The input layer consists of tool rotational speed, welding speed, tool shoulder and pin radius, pin length and axial force. The responses include peak temperature, total torque, traverse force, bending stress and maximum shear stress. Since the pin length is usually considered as 90% of the plate thickness in many FSW operations to obtain full penetration, the plate thickness is not considered as an additional variable. A separate neural network model is developed for each response variable. The hidden layer in each neural network model has a variable number of nodes depending on the non-linearity of the relationship between the input variables and the selected response variable.

The input variables are connected to the output of the model via the nodes in the hidden layer (Fig. 1). The output of a node is computed using a hyperbolic tangent function as

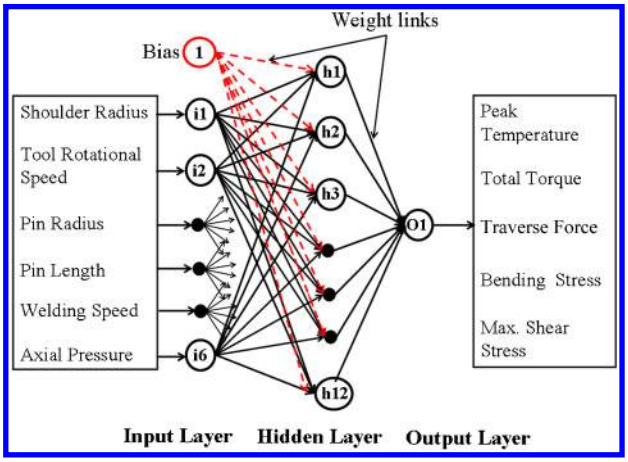

1 Architecture of proposed ANN models

$$y = \tanh\left(\sum_{i=1}^{n} w_i x_i + \theta_i\right) \tag{5}$$

where y is the output of a node, x_i is the input, w_i is the weight, θ_i is the bias attached to the ith input node and n is the total number of nodes contributing to the specific output node in the hidden or output layer. The ANN models are trained in batch mode following the feed forward back propagation algorithm with Bayesian approach that allows the estimation of uncertainty in the predictions. The weights for each ANN model are optimised by minimising the objective function E as[27–29]

$$E = \frac{\beta}{n} E_D + \frac{\alpha}{m} E_W \tag{6}$$

where β and α are two regulariser terms related to the noise in the data set and uncertainty in the distribution of weights respectively, n is the number of data sets and m is the total number of weights in a neural network model. The terms E_D and E_W refer to the error in data sets and weight distributions and are expressed as[27–29]

$$E_D = \frac{1}{2}\left[\sum_{i=1}^{n} (d_i - y_i)^2\right] \tag{7}$$

$$E_W = \frac{1}{2}\sum_{j=1}^{m} w_j^2 \tag{8}$$

where d_i and y_i are the desired and corresponding estimated outputs for the ith data set respectively. The weights are updated as[30]

$$w_{k+1} = w_k - \left[\eta\left(\frac{\partial E}{\partial w}\right)_{k+1} + \varphi\left(\frac{\partial E}{\partial w}\right)_k\right] \tag{9}$$

where η and φ refer to the learning rate and momentum transfer constant respectively, and w_{k+1} and w_k refer to the weights in two successive iterations $k+1$ and k. The regulariser terms β and α are also updated in every iteration as[27–29]

$$\beta = \frac{m-\gamma}{2E_D} \tag{10}$$

$$\alpha = \frac{\gamma}{2E_W} \tag{11}$$

The term γ is referred to the effective number of parameters in a neural network model and is expressed as $\gamma = m - \alpha \times \text{trace}(H)^{-1}$, where H is a Hessian matrix and computed as[27–29]

$$H = \beta\nabla^2 E_D + \alpha\nabla^2 E_W \tag{12}$$

For a given data set, several neural network models with the number of hidden nodes varying from 6 to 12 (twice the number of input nodes) are trained and compared based on the respective log predictive error that is computed as[30]

$$\text{LPE} = \frac{\beta}{2}\sum_{i=1}^{n} (d_i - y_i)^2 + \frac{n}{2}\ln\left(\frac{2\pi}{\beta}\right) \tag{13}$$

The neural network model with the least log predictive error is selected as the best and is expected to provide a balance between over- or underfitting and the complexity of model. The uncertainty of the predictions from the neural network model is calculated as[29,31]

$$\sigma = \left\{\frac{1}{\beta} + \left[\frac{\partial y_i}{\partial w_j}\right]^T [H]^{-1} \left[\frac{\partial y_i}{\partial w_j}\right]\right\}^{1/2} \tag{14}$$

In equation (14), the first term on the right hand side refers to the variance due to noise in the data set, and the second term indicates the error due to sensitivity of the prediction on the weight distribution. The following web sites host further description of the theory for the construction of ANN models, the computer code used, a user's manual for the ANN model and the complete data sets used for the

Table 1 Levels of six input variables used for training and testing of ANN models for FSW of AA 7075

Input variable	Shoulder radius/ $\times 10^{-2}$m	Pin radius/ $\times 10^{-2}$m	Pin length/ $\times 10^{-2}$m	Welding speed/ $\times 10^{-2}$ m s^{-1}	Rotational speed/ rev min^{-1}	Axial pressure/ MPa
Levels for training (L50)	0·75	0·200	0·27	0·1	300	18
	1·00	0·225	0·35	0·2	420	20
	1·25	0·250	0·43	0·3	570	22
	1·50	0·275	0·55	0·4	750	25
	1·75	0·300	0·93	0·5	900	27
Levels for training (CCD)	0·75	0·25	0·27	0·1	300	18
	0·99	0·28	0·41	0·23	494	22·53
	1·1	0·30	0·5	0·3	600	25
	1·26	0·32	0·56	0·37	706	27·47
	1·5	0·35	0·7	0·5	900	32
Levels for testing (L50)	0·9	0·21	0·306	0·15	360	19
	1·1	0·24	0·387	0·25	480	21
	1·3	0·26	0·468	0·33	630	23
	1·4	0·27	0·513	0·36	680	24
	1·6	0·29	0·594	0·45	820	26

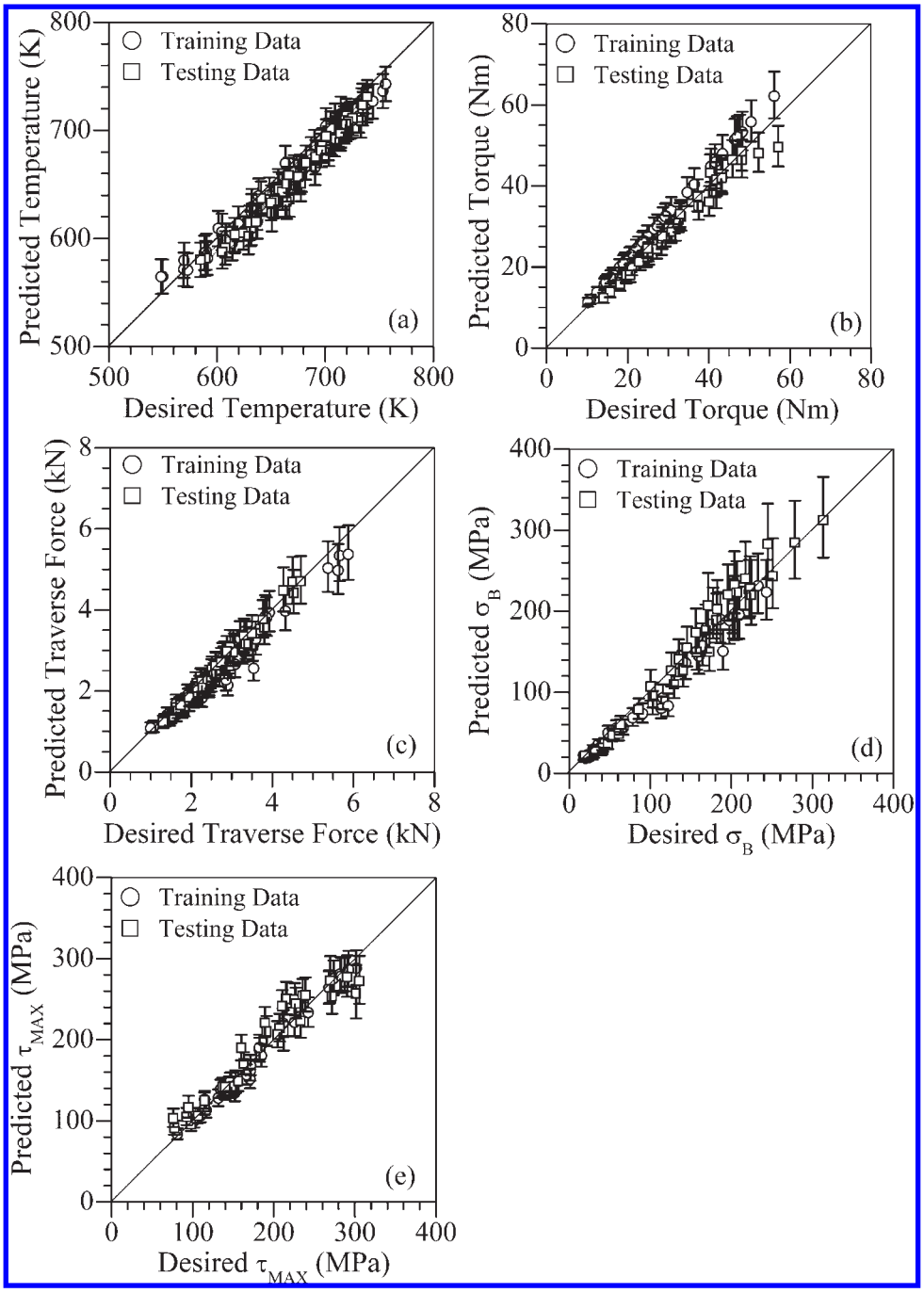

2 Desired (from numerical model) *vis-à-vis* estimated (from neural network models) values of *a* peak temperature, *b* torque, *c* traverse force, *d* bending stress σ_B and *e* maximum shear stress τ_{MAX}

training and testing of the ANN models. http://www.me.iitb.ac.in/~amit/ANN; http://www.matse.psu.edu/modeling/ANN

Results and discussions

Performance of ANN models

The range of training and testing data sets is presented in Table 1. The FSW of 0·003–0·007 m thick AA 7075 plates with tool shoulder radius ranging from 0·0075 to 0·0175 m, pin radius from 0·002 to 0·003 m, welding speed from 0·001 to 0·005 m s^{-1}, rotational speed from 300 to 900 RPM and axial pressure from 18 to 27 MPa is considered. The length of the tool pin in Table 1 relates to the plate thickness. The ranges of the computed values of response variables corresponding to several combinations of welding conditions are as follows. The peak temperature varies from 560 to 760 K. The total torque and the traverse force experienced by the tool vary from 10 to 60 Nm and from 1·0 to 6·0 kN respectively. The bending stress and the resultant maximum shear stress experienced by the tool pin range from 20 to 300 and 70 to 300 MPa respectively. Similar ranges of these response variables are observed by both model calculations and actual experiments reported in the literature.[4–13] The complete training and testing data sets are uploaded separately as Supplementary Material 1 http://dx.doi.org/10.1179/1362171812Y.0000000035.s1 in the journal homepage.

Figure 2*a–e* shows the performance of the five ANN models in predicting the response variables, e.g. peak temperature, and the torque, traverse force, bending stress and maximum shear stress experienced by the tool

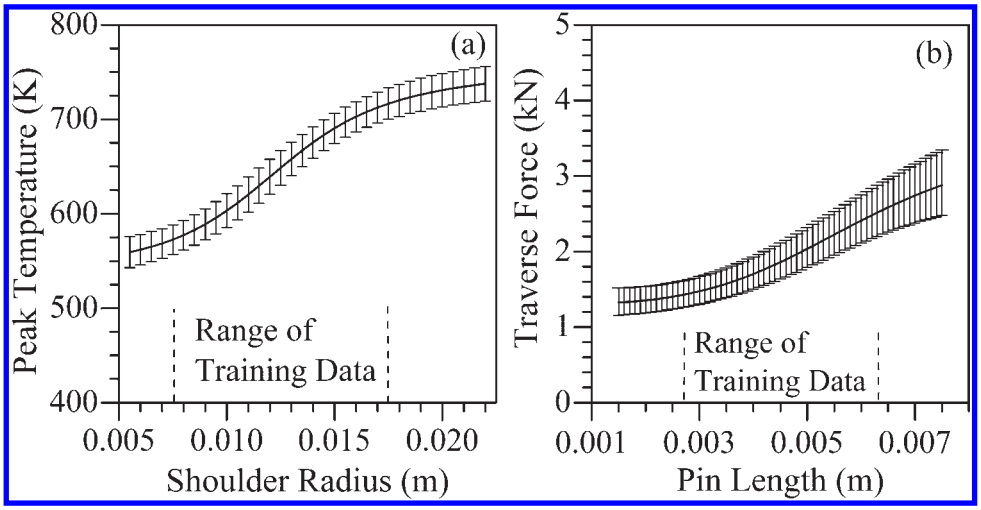

a pin radius: 0·0022 m, pin length: 0·003 m, welding speed: 0·001 m s^{-1}, rotational speed: 400 rev min^{-1}, axial pressure: 20 MPa; *b* shoulder radius: 0·0075 m, pin radius: 0·0025 m, welding speed: 0·001 m s^{-1}, rotational speed: 300 rev min^{-1}, axial pressure: 18 MPa

3 Prediction of *a* peak temperature as function of shoulder radius and *b* traverse force as function of pin length: other conditions corresponding to *a* and *b* are as follows

using both training and testing data sets. The numbers of hidden nodes in the final ANN models range from 9 to 11, which indicate complex interrelations between each response variable and the welding conditions and tool geometry. The error bars in Fig. 2 depict the uncertainties in the prediction of the response variables with 95% level of confidence for various welding conditions. Figure 2 shows a fair agreement between the predicted and desired values of response variables with the errors in prediction ranging from $\pm 2{\cdot}5\%$ for peak temperature, $\pm 7{\cdot}5\%$ for torque, traverse force and maximum shear stress and up to $\pm 12\%$ for bending stress. The errors tend to increase in the region with sparse population of training data sets. For example, the uncertainty in the prediction of bending stresses increases beyond 250 MPa since the training data sets contain very few welding conditions, resulting bending stresses of >250 MPa.

Distribution of error bars in ANN model predictions

Figure 3*a* shows the estimated values of peak temperature and its uncertainty in prediction as a function of tool shoulder radius for welding conditions beyond $\pm 20\%$ of the range of the training data sets. Similarly, Fig. 3*b* shows the estimated values of traverse force and its uncertainty in prediction as a function of pin length for welding conditions beyond $\pm 20\%$ of the range of the training data sets. Figure 3*a* shows that the peak temperature increases with the tool shoulder radius. For larger shoulder radius, the higher surface area at the tool/workpiece interface results in greater heat generation rate and higher peak temperature. Figure 3*b* shows that the traverse force increases with longer pins used for the welding of thicker plates. For a given welding condition, the increase in plate thickness reduces the peak temperature and forces the tool pin to push a larger volume of cooler and stronger workpiece material. Figure 3*a* and *b* shows that the optimised ANN models are able to predict the variations of peak temperature as a function of tool shoulder radius and traverse force as function of pin length even for values that are well beyond the range of training data sets in each case. However, the uncertainty in the predictions increases beyond the range of training data sets.

The performance of the ANN model for peak temperature is examined for input variables other than shoulder radius $\pm 20\%$ beyond the ranges of the training data sets. Although the ANN model has been able to capture the trend in the variation of peak temperature as a function of the input variables fairly well, the uncertainty in prediction increases up to $\pm 4\%$ in cases when the input variables are considered beyond the range of the training data set by $\pm 20\%$. In contrast, the uncertainty in prediction in temperature lies within $\pm 2{\cdot}5\%$ of the predicted values when the input variables are considered within the training range. Similar examination of the ANN model for the traverse force resulted in uncertainty of prediction up to $\pm 18\%$ of the predicted values for welding variables exceeding the range of training data by $\pm 20\%$. In contrast, the maximum uncertainty in the prediction of traverse force remains within $\pm 15\%$ of the predicted values for within the range of the training data sets. The ANN models for the prediction of torque, bending stress and maximum shear stress exhibited uncertainties in predictions up to ± 12, ± 20 and $\pm 12\%$ of the predicted values respectively in the range $\pm 20\%$ beyond the training data set. In contrast, the uncertainties in prediction remained within ± 8, ± 17 and $\pm 8\%$ of the predicted values for the ANN models for the torque, bending stress and maximum shear stress respectively in the range of the training data set values shown in Table 1.

The uncertainty in the predicted values of peak temperature is considerably lower than that in the computed values of the other four variables. Since temperature affects the material properties and many other intermediate variables, any uncertainty in temperature augments to the inherent uncertainty in the calculation of the other variables, increasing the overall uncertainty. Since the peak temperature is a key variable in FSW, the ability of the neural network to estimate its value fairly accurately makes the ANN model particularly useful.

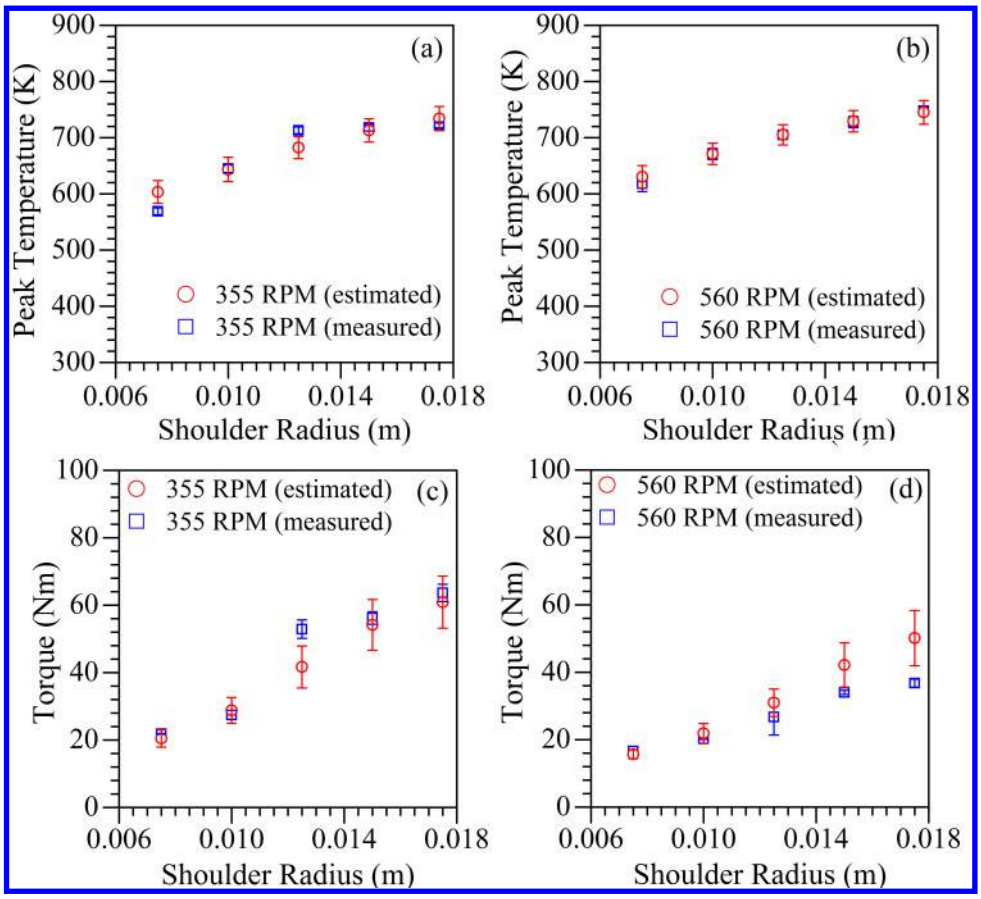

4 Comparison of experimentally measured and estimated (using optimised neural networks) values of *a*, *b* peak temperature and *c*, *d* torque experienced by tool: welding conditions and tool geometry corresponding to experimentally measured values are as follows (pin radius: 0·003 m at root to 0·00233 m at bottom, pin length: 0·003325 m, welding speed: 0·00067 m s^{-1} and axial pressure: 30 MPa)

Validation of ANN model predictions with experimental results

Figure 4*a*–*d* shows comparisons between the values of peak temperature and torque computed from the ANN models with the corresponding measured values[10] for the FSW of AA 7075. It can be noted that the measured values of the temperatures were at a transverse distance of 0·0085 m from the butting surface (on the retreating side) and a depth of 0·00075 m from the top surface during FSW of 0·0035 m thick AA 7075.[10] Figure 4*a* and *b* shows that the values calculated from the optimised ANN models agree fairly well with the corresponding experimental results for various values of shoulder radius and tool revolutions per minute. The peak temperature increases significantly with the increase in tool shoulder radius and gently with the increase in tool rotational speed. A larger tool shoulder radius results in greater heat generation rate and higher peak temperature at the interface between the tool shoulder and the workpiece. An increase in tool rotational speed also results in a higher rate of heat generation and greater peak temperature. Figure 4*c* and *d* show that the torque experienced by the tool increases with the increase in tool shoulder radius and decrease in tool rotational speed. The increase in the tool–workpiece contact area with the increase in tool shoulder radius leads to greater torque requirement. The increase in tool rotational speed increases the slip along the tool/workpiece interface, reducing the overall torque experienced by the tool. Figure 4*c* and *d* also indicates a fair agreement between the measured values of torque and the corresponding estimated values from the optimised neural network models. It is noteworthy that the welding speed and the axial force for the experimentally measured results are beyond the ranges of the training data used, but they did not exceed the range beyond $\pm 20\%$. Thus, even when the peak temperature and torque exceeded the training data set range by $\pm 20\%$, the ANN models are able to capture their respective values and trends fairly well.

Conclusions

Five ANN models are developed following the Bayesian approach for the calculation of peak temperature, traverse force, torque, bending stress and maximum shear stress experienced by the tool during FSW of AA 7075. The input welding variables included tool shoulder radius, tool rotational speed, pin radius and pin length, welding speed and axial force. The training and testing data sets for the ANN models are obtained from a well tested comprehensive 3D heat transfer and material flow model for FSW. The optimised ANN models have shown fairly good performance in predicting the corresponding response variables. The uncertainties in the prediction from the ANN models vary from $\pm 2{\cdot}5\%$ for peak temperature to $\pm 7{\cdot}5\%$ for torque, traverse force and maximum shear stress, and up to $\pm 12\%$ for the bending stress within the range of the training data. When the values are calculated exceeding

up to $\pm 20\%$ of the range of the training data sets, the maximum values of such uncertainties in prediction were $\pm 4\%$ for peak temperature, $\pm 12\%$ for torque and the maximum shear stress, $\pm 15\%$ for traverse force and $\pm 20\%$ for the bending stress. The optimised neural network models for temperature and torque can predict the trends and values of the available experimental data fairly well. The five neural networks, valid for the tool–material combinations within the range of independent variables indicated in Table 1, are available from web sites indicated in the paper.

References

1. H. K. D. H. Bhadeshia and T. DebRoy: *Sci. Technol. Weld. Join.*, 2009, **14**, (3), 193–196.
2. T. DebRoy and H. K. D. H. Bhadeshia: *Sci. Technol. Weld. Join.*, 2010, **15**, (4), 266–270.
3. R. Heideman, C. Johnson and S. Kou: *Sci. Technol. Weld. Join.*, 2010, **15**, (7), 597–604.
4. P. A. Colegrove, H. R. Shercliff and R. Zettler: *Sci. Technol. Weld. Join.*, 2007, **12**, (4), 284–297.
5. R. Nandan, G. G. Roy, T. Lienert and T. DebRoy: *Sci. Technol. Weld. Join.*, 2006, **11**, (5), 526–537.
6. R. Nandan, B. Prabu, A. De and T. DebRoy: *Weld. J.*, 2007, **86**, 231s–240s.
7. R. Nandan, T. J. Lienert and T. DebRoy: *Int. J. Mater. Res.*, 2008, **99**, (4), 434–444.
8. A. Arora, R. Nandan, A.P. Reynolds and T. DebRoy: *Scr. Mater.*, 2009, **60**, 13–16.
9. A. Arora, A. De and T. DebRoy: *Scr. Mater.*, 2011, **64**, (1), 9–12.
10. M. Mehta, A. Arora, A. De and T. DebRoy: *Metall Trans. A*, 2011, **42A**, (9), 2716–2722.
11. A. Arora, T. DebRoy and H. K. D. H. Bhadeshia: *Acta Mater.*, 2011, **59**, (5), 2020–2028.
12. G. G. Roy, R. Nandan, and T. DebRoy: *Sci. Technol. Weld. Join.*, 2006, **11**, (5), 606–608.
13. R. Nandan, T. DebRoy and H. K. D. H. Bhadeshia: *Prog. Mater. Sci.*, 2008, **53**, 980–1023.
14. H. K. D. H. Bhadeshia: *ISIJ Int.*, 1999, **39**, (10), 966–979.
15. H. K. D. H. Bhadeshia, R. C. Dimitriu, S. Forsik, J. H. Pak and J. H. Ryu: *Mater. Sci. Technol.*, 2009, **25**, (4), 504–510.
16. S. Mishra and T. DebRoy: *Mater. Sci. Eng. A*, 2007, **A454**–**A455**, 477–486.
17. L. Fratini, G. Buffa and D. Palmeri: *Comput. Struct.*, 2009, **87**, (17–18), 1166–1174.
18. L. Fratini and G. Buffa: *J. Eng. Mater. Technol. – Trans. ASME*, 2008, **130**, (3), 031001.
19. P. A. Fleming, D. H. Lammlein, D. M. Wilkes, G. E. Cook, A. M. Strauss, D. R. DeLapp and D. A. Hartman: *Sci. Technol. Weld. Join.*, 2009, **14**, (1), 93–96.
20. E. Boldsaikhan, E. M. Corwin, A. M. Logar and W. J. Arbegas: *Appl. Soft Comput.*, 2011, **11**, (8), 4839–4846.
21. M. K. Kulekci, U. Esme, O. Er and Y. Kazancoglu: *Materialwiss. Werkstofftech.*, 2011, **42**, (11), 990–995.
22. A. K. Lakshminarayanan and V. Balasubramanian: *Trans. Nonferrous Met. Soc. China*, 2009, **19**, (1), 9–18.
23. U. Esme, M. K. Kulekci and Y. Kazancoglu: *J. Adv. Mater.*, 2010, **42**, (4), 14–21.
24. H. Okuyucu, A. Kurt and E. Arcaklioglu: *Mater. Des.*, 2007, **28**, (1), 78–84.
25. A. Arora, M. Mehta, A. De and T. DebRoy: *Int. J. Adv. Manuf. Technol.*, 2012, DOI: 10.1007/s-00170-011-3759-7.
26. D. C. Montgomery: 'Design and analysis of experiments', 7th ed; 2009, New York, John Wiley & Sons Inc.
27. D J. C. MacKay: *Neural Comput.*, 1992, **4**, 448–472.
28. C. M. Bishop: 'Neural networks for pattern recognition', Indian edn, 150–152, , 385–433; 2009, Oxford, Oxford University Press.
29. V. Narayan, R. Abad, B. Lopez, H. K. D. H. Bhadeshia and D. J. C. MacKay: *ISIJ Int.*, 1999, **39**, (10), 999–1005.
30. C. G. Chua and A. T. C. Goh: *Int. J. Numer. Anal. Methods Geomech.*, 2003, **27**, 651–667.
31. R. P. Cherian, P. S. Midha and A. G. Pipe: *Int. J. Prod. Res.*, 2000, **38**, (10), 2201–2214.